CEAS-GNC-2022-001

CEAS EuroGNC 2022
"Conference on Guidance, Navigation and Control"
3-5 May 2022 @ Technische Universität Berlin, Germany

Performance Assessment of an Extremum Seeking Controller Using Continuation Methods

Duc H. Nguyen Research & Teaching Associate, University of Bristol, Department of Aerospace Engineering, BS8 1TR, Bristol, United Kingdom. duc.nguyen@bristol.ac.uk

Mark H. Lowenberg Professor of Flight Dynamics, University of Bristol, Department of Aerospace Engineering, BS8 1TR, Bristol, United Kingdom. m.lowenberg@bristol.ac.uk

Simon A. Neild Professor of Nonlinear Structural Dynamics, University of Bristol, Department of Aerospace Engineering, BS8 1TR, Bristol, United Kingdom. simon.neild@bristol.ac.uk

ABSTRACT

Assessing the performance of extremum seeking control – a class of model-free adaptive controller – remains a mathematically-intensive task that involves many restrictive assumptions due to the presence of a harmonic forcing signal. In this paper, we propose the use of bifurcation analysis and numerical continuation to provide a simple numerical framework for engineers to investigate the dynamics of an extremum seeking system. Using the example of a poorly-tuned auto-trim system on a nonlinear airliner model, the advantage of bifurcation analysis and continuation is demonstrated, including the ability to directly identify the oscillation amplitude and stability information. Other behaviours common in nonlinear harmonically-forced systems, such as existence of multiple solutions and bifurcations leading to multi-harmonic responses, are also detected. The purpose of this paper is to demonstrate the advantages of continuation in characterising the dynamics of an extremum seeking controller and to present this exciting controller scheme to the wider aeronautics audience.

Keywords: extremum seeking, harmonic forcing, bifurcation analysis, dynamical systems

Nomenclature

A	=	forcing amplitude	J	=	objective function
c	=	mean aerodynamic chord	K_E	=	learning rate (a proportional gain)
C_x, C_z, C_m	=	force and moment coefficients	m	=	mass
g	=	gravitational acceleration	q	=	pitch rate
h	=	thrust line distance above CG	S	=	wing area
I_y	=	pitch moment of inertia	t	=	time

V	=	total velocity	θ	=	pitch angle
α	=	angle of attack	ρ	=	air density
δ_e	=	elevator deflection	φ	=	phase lag
δ_t	=	tailplane deflection	ω	=	forcing frequency

1 Introduction

Extremum seeking control is a form of model-free adaptive control that automatically seeks out the extremum point(s) (maxima or minima) of an objective function. This is done via a 'perturb and observe' scheme, which injects a sinusoidal perturbation to the control signal and observes the subsequent changes in the objective function. An online estimation of the objective function's slope can then be inferred, which in turn drives the control input to the point at which the slope is zero (i.e., the extremum). As the whole process is done online and does not require any knowledge of the plant, extremum seeking control is especially useful in cases where the optimal set point is either not known or is highly sensitive to changes in parameters, as often seen in many real-world applications.

Extremum seeking control has attracted significant attention from researchers in recent years. Specifically, the number of publications on the topic between 2000 and 2009 alone exceeded those from the year 1960 to 2000 combined [1]. Part of the reason for this sudden surge in interest is due to a pivotal paper in 2000, which provided the first rigorous mathematical proof of stability in a general nonlinear extremum-seeking system [2]. Since then, various engineering and industrial applications of extremum seeking control has been explored, including internal combustion engine [3], wind power systems [4], and for optimising formation flight [5], to name a few. On the theoretical front, some notable works include automatic tuning of PID gains [6], limit cycle amplitude minimisation [7], convergence analysis [8], and optimising systems with only periodic solutions [9]. Another recent development is the addition of a built-in extremum-seeking controller block in the R2021a release of the Simulink Control Design toolbox in MATLAB [10]. This reflects the increasing popularity of the method and will further introduce extremum seeking control to many new users through a user-friendly environment. For more background on the theories as well as applications of extremum seeking control in other fields, readers are referred to papers [1, 11] and textbooks [12, 13].

Despite these developments, the current procedures for analysing an extremum-seeking system remain mathematically challenging and involve a number of assumptions that may prove impractical in many engineering systems. This in large part is due to the presence of the harmonic perturbation, which results in periodic motions and poses a major challenge to both analytical and numerical analyses. Regarding the analytical side, the method of averaging and the singular perturbation method are employed to reduce the system under investigation and approximate it as an equilibrium map [2]. The assumptions involved in these approaches require that the frequencies of the three main elements (the perturbation signal, the filters in the extremum controller, and the plant's dynamics) are well-separated [7] – usually by an order of magnitude each. Considering the example of a generic flight dynamics model, these requirements are already limiting since a simple longitudinal (4^{th}-order) aircraft model with actuator already spans three orders of magnitude on the frequency spectrum: 10^{-1}-10^{0} rad/s for the two rigid-body modes and 10^{1} rad/s for the actuator. The impact of higher-order harmonic terms is also neglected in these approximations, which may further invalidate the results in highly nonlinear applications. On the numerical front, recent works have successfully employed numerical continuation using the AUTO-07P software to analyse extremum seeking controllers [14-17]. Various nonlinear phenomena have been characterised using this continuation-based scheme, including existence of multiple stable solutions,

unstable solutions, and loss of stability. However, the underlying equations used by the numerical solver in [14-17] are still equilibrium approximations of the full harmonically-forced systems, so the limitations listed above still apply.

To fill in this gap, we present here an example of how harmonically-forced bifurcation analysis can be employed to analyse an extremum seeking controller on a highly nonlinear system with no closed-form solutions. This method effectively converts the harmonically-forced plant into an autonomous self-oscillating system, which can then be easily solved by continuation. Past applications of harmonically-forced bifurcation analysis have focused on examining the frequency response of nonlinear systems, most famously the Duffing equation (see section II in [18] for a brief introduction), along with some recent developments in the field of flight dynamics and control [18, 19]. In presenting this work, we hope that the combination of bifurcation analysis and extremum seeking control will provide a powerful framework for future researchers and engineers to design and test many advanced implementations of this controller scheme. The example problem shown here can also be another contribution to the ever-expanding literature on dynamics of nonlinear harmonically-forced systems.

2 Problem Description

In this paper, we consider a fourth-order longitudinal aircraft model coupled with a conventional manoeuvre-demand controller and an auto-trim system – the latter uses extremum seeking. Although both controllers provide stability and accomplish their objectives, they have been intentionally tuned to achieve poor performance. This provides the backdrop to demonstrate the capability of harmonically-forced bifurcation analysis in identifying the stability boundaries and revealing the wide variety of dynamics that can be encountered in a poorly-designed controller or on a highly nonlinear plant.

2.1 Aircraft Model and the Manoeuvre-Demand Controller

The open-loop equations of motion for the longitudinal rigid-body modes of an aircraft can be written

$$\dot{\alpha} = \frac{1}{mV}\left[\frac{1}{2}\rho V^2 S(C_z \cos\alpha - C_x \sin\alpha) - T\sin\alpha + mg\cos(\theta-\alpha)\right] + q \tag{1}$$

$$\dot{V} = \frac{1}{m}\left[\frac{1}{2}\rho V^2 S(C_z \sin\alpha + C_x \cos\alpha) + T\cos\alpha - mg\sin(\theta-\alpha)\right] \tag{2}$$

$$\dot{q} = \frac{1}{2}\rho V^2 Sc\frac{C_m}{I_y} - \frac{Th}{I_y} \tag{3}$$

$$\dot{\theta} = q \tag{4}$$

in which the coefficients of aerodynamic force along the body x and z axes C_x and C_z (forwards along the fuselage and downwards respectively) and the moment coefficient in pitch C_m are represented as follows:

$$C_i = C_{i_0}(\alpha) + C_{i_1}(\alpha, \delta_e, \delta_s) + C_{i_2}(\alpha)\frac{cq}{2V} \tag{5}$$

where $i = [x, z, m]$. Standard flight dynamics notation is used – see nomenclature. These coefficients are shown in Fig. 2, depicting data from the NASA Generic T-tail Model (GTT – see Fig. 1) – created to

represent a generic mid-sized regional airliner. pchip and spline interpolation/extrapolation are used to make the model smooth, which is beneficial for bifurcation analysis. Numerical values for the remaining parameters in equations (1-5) are listed in Table 1.

Fig. 1 The NASA GTT

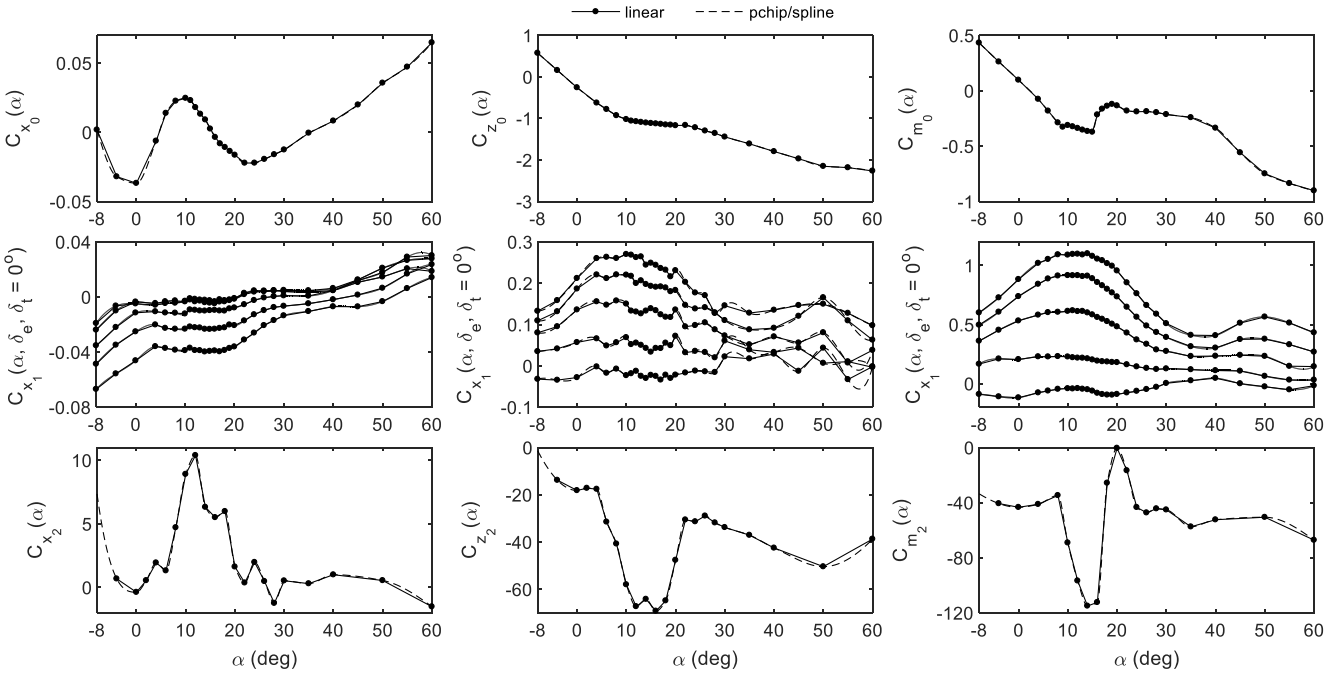

Fig. 2 Aerodynamic coefficients of the GTT

Table 1 Aircraft parameters

S	wing area	70.1 m^2	ρ	air density (at 10,000 ft)	0.905 kg/m^3
c	mean aerodynamic chord	3.37 m	I_y	pitch moment of inertia	1,510,624 kg m^2
h	engines' height above CG	2.02 m	g	gravitational acceleration	9.81 m/s^2
m	mass	25,332 kg	T	thrust	29,982 N

A simple angle-of-attack demand controller as shown in Fig. 3 is used in our analysis. The reference input is demanded angle of attack α_d, which is subtracted from the actual angle of attack in the outer loop and then integrated. In the inner loop, a proportional stability augmentation system is included using pitch rate q and pitch angle θ feedback. All three gains K_I, K_q, and K_θ are fixed gains.

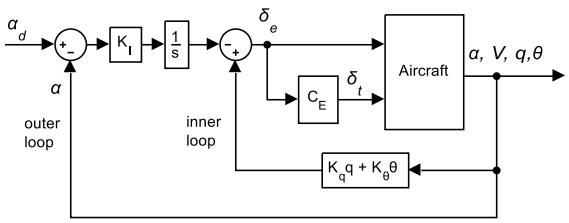

Fig. 3 Closed-loop block diagram

The block C_E is the extremum-seeking controller used for auto-trim. Its input is the elevator deflection δ_e and the output is tailplane deflection δ_t. The details of its working are presented in the next section. As mentioned, the closed-loop system is stable, although the gains have been selected to give poor performance.

2.2 The Extremum-Seeking Auto-Trim Controller

An extremum-seeking controller will automatically seek out the maxima or minima of an objective function, which are the points with zero slopes. In this example, the objective function is set to be $J = |\delta_e|$. The idea is that controller will adjust the tailplane deflection until $|\delta_e|$ reaches its minimum at zero. When this condition is achieved, the aircraft will be flying at the commanded angle of attack using only tailplane for trim and may represent minimum drag trim for the specific flight condition.

The static relationship between elevator and tailplane deflections to keep the aircraft in trimmed flight at 2 deg angle of attack is shown as the solid line in Fig. 4a, with the inset showing a magnified view. Only aerodynamic data for tailplane between –10 and +5 deg are available. However, they can be spline-extrapolated as shown by the dashed lines. This artificially creates a peak and a trough with zero slopes that can potentially draw the auto-trim controller toward them instead of the desired $|\delta_e|$ = 0 point. For our purpose, this artificial peak/trough pair is desirable as it allows us to demonstrate the full capability of continuation methods in identifying additional attractors that may be hard to detect. Therefore, spline extrapolation is used for the tailplane aerodynamic data. This results in the objective function $J = |\delta_e|$ as shown in Fig. 4b, with the three zero-slope points labelled A-C; point A is the desired target for the auto-trim controller.

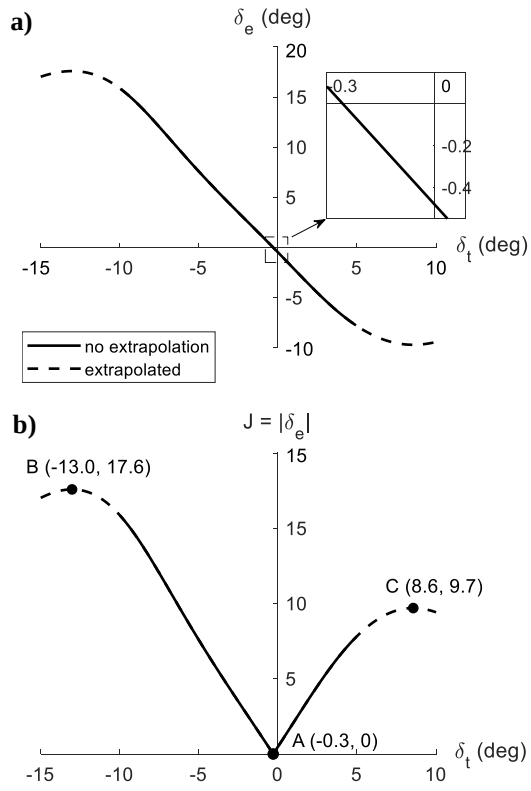

Fig. 4 Static relationship between elevator and tailplane at trim for flight at α = 2º (a) and the objective function (b).

A brief introduction to the principles extremum seeking control is now presented, although readers are referred to sources such as [12, 13] for a more formal introduction. Fig. 5 is the block diagram of the auto-trim controller – previously labelled simply as C_E in Fig. 3. The input to the controller is elevator, which is automatically controlled by the α-demand system. $J = |\delta_e|$ is the objective function as

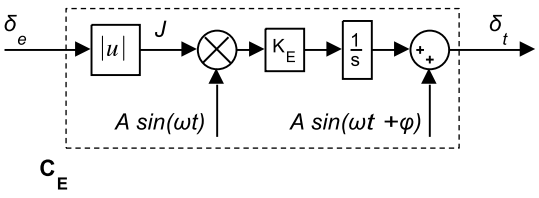

Fig. 5 Block diagram of the auto-trim controller.

defined. This signal is multiplied by a sinusoidal perturbation of the form $A\sin(\omega t)$ and a proportional gain K_E and then integrated. Finally, another sinusoidal perturbation is added with a phase lag φ, giving us the tailplane deflection. In this scheme, the controller will continuously perturb the tailplane δ_t at a frequency ω rad/s, thereby causing J to vary sinusoidally at the same frequency. Due to the presence of the α-demand controller, J will follow the static map shown in Fig. 4 in response to changes in the set point of δ_t. This set point is controlled by the integral action, which continuously drives δ_s until $JK_EA\sin(\omega t)$ oscillates symmetrically about zero. This only happens when J reaches one of the inflection points in Fig. 4 (so that the product of $J(\omega t)$ and $\sin(\omega t)$ is symmetric about zero). The extremum seeking controller therefore has the capability to automatically seek out an inflection point in an objective function without any knowledge of the model – making it especially useful for plants that are sensitive to changes in system parameters. We acknowledge that a real-world auto-trim controller does not require extremum seeking [20-22] and the example provided here is only to exemplify the capability of bifurcation and continuation methods in analysing an extremum-seeking system. Table 2 shows the parameters of the auto-trim controller used in this paper.

Table 2 Extremum seeking controller parameter

A	forcing amplitude	0.2 deg
K_E	learning rate	5 rad/s
ϕ	demodulation phase	90 deg

The effects of both the α-demand and the auto-trim controllers are now presented. Fig. 6 shows the aircraft responding to a step change in demanded angle of attack from 1 to 2 deg using two different forcing frequencies – both are under 1 Hz and can therefore be considered realistic. In both instances, the angle of attack converges to its commanded value of 2 deg. However, the second case with 4 rad/s forcing fails to drive the elevator to zero, and instead converges to the inflection point C in Fig. 4. This does not happen when ω is increased to 6 rad/s, as seen in Fig. 6a. In practice, performance can be improved by better tuning of both the α-demand and the auto-trim controllers, as well as the addition of a low-pass and/or high-pass filter in the extremum controller. The use of filters is not discussed here.

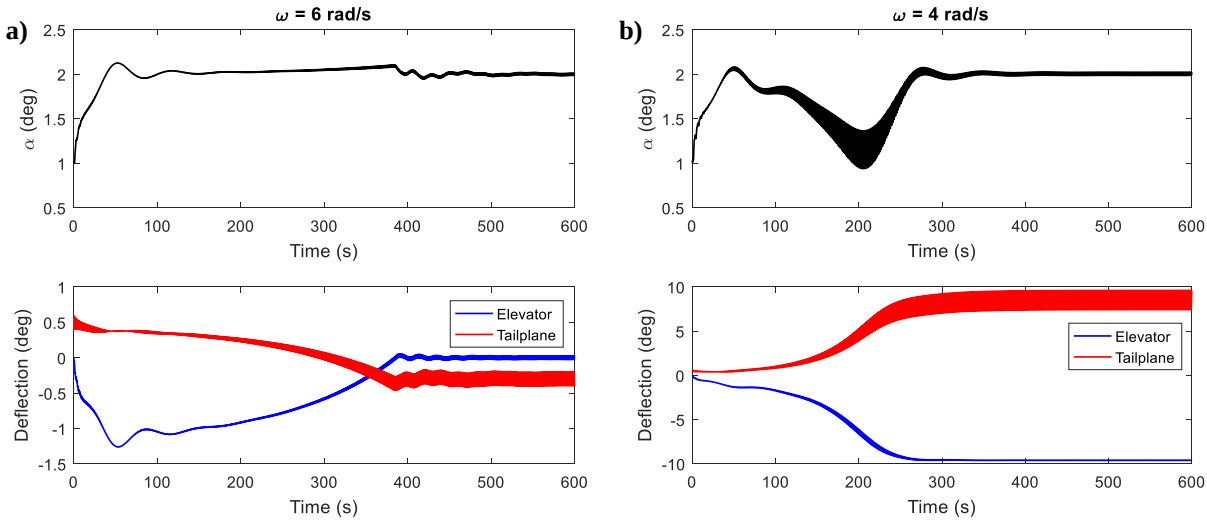

Fig. 6 Step responses in α_d using two different forcing frequencies.

3 Harmonically-Forced Bifurcation Analysis

Having discussed the basics of extremum control and its potential shortcomings in highly nonlinear applications, we now propose the use of bifurcation analysis and numerical continuation as a tool to systematically assess the performance in those situations. Since its first application to flight dynamics models in the early 80s [23, 24], bifurcation analysis has seen increasing use in the field of aircraft dynamics and control by both the research community and the industry [25]. This method traces out a map of equilibrium and limit cycles solutions – both stable and unstable – in a nonlinear system in response to static changes in an input parameter (such as control surface deflection). Past studies have successfully used bifurcation analysis to characterise various nonlinear behaviours of interests such as spin, wing rock, and jump phenomenon [26], as well as to assess the performance of flight control systems [27, 28]. These studies, however, were still restricted to analysing quasi-static changes to the input parameter. A further extension the method in the flight dynamics context has been proposed recently, which permits examinations of the aircraft's responses to a harmonic forcing input; the results are then presented in the form of a nonlinear Bode plot [18, 19]. The same approach is used here to analyse a closed-loop system with an extremum seeking controller, which is inherently periodic due to the presence of the sinusoidal perturbation. We will refer to this approach as harmonically-forced bifurcation analysis in this paper.

The method to implement harmonically-forced bifurcation analysis in an extremum-seeking system is now presented. In general, bifurcation analysis requires that the state equations be written as autonomous first-order ordinary-differential equations. The harmonic forcing term $\sin \omega t$ (or other equivalent) can be generated in such an environment by the addition of two 'dummy states'

$$\begin{aligned} \dot{x}_1 &= \quad x_1 + \omega x_2 - x_1(x_1^2 + x_2^2) \\ \dot{x}_2 &= -\omega x_1 + x_2 - x_2(x_1^2 + x_2^2) \end{aligned} \tag{6}$$

It can be shown that $x_1 = \sin \omega t$ and $x_2 = \cos \omega t$ are asymptotically stable solutions of equation (6). These two states can now be used to generate the harmonic forcing signals in an extremum seeking controller. Accordingly, the whole plant is now a self-oscillating autonomous system, for which steady state solutions can be found by continuation in the same way as an autonomous (non-forced) system can be solved for limit cycle solutions.

All bifurcation analysis in this paper was done in the MATLAB/Simulink environment using the Dynamical Systems Toolbox [29], which is the MATLAB implementation of the continuation software AUTO-07P [30].

4 Results

4.1 Existence of Multiple Solutions

The two different responses observed in Fig. 6 suggest that there are at least two stable solutions at 4 rad/s forcing. Using these two responses as starting points for the continuation solver, the resulting bifurcation diagrams of the elevator and tailplane deflections are shown in Fig. 7. The forcing frequency ω is set as the continuation parameter, thereby giving us an indication of how our choice of ω affects the

oscillation amplitude and stability. All solutions in Fig. 7 are periodic, and both the maxima and the minima of the oscillation are shown (note that in some cases, including much of the stable solution for elevator, the amplitudes are small and the maxima and minima are indistinguishable in the figure). Therefore, the oscillation amplitudes are easily indentified on the diagram – a major advantages over existing methods that approximate the responses as equilibrium maps. For the rest of the paper, only stable solutions are discussed in the interests of brevity.

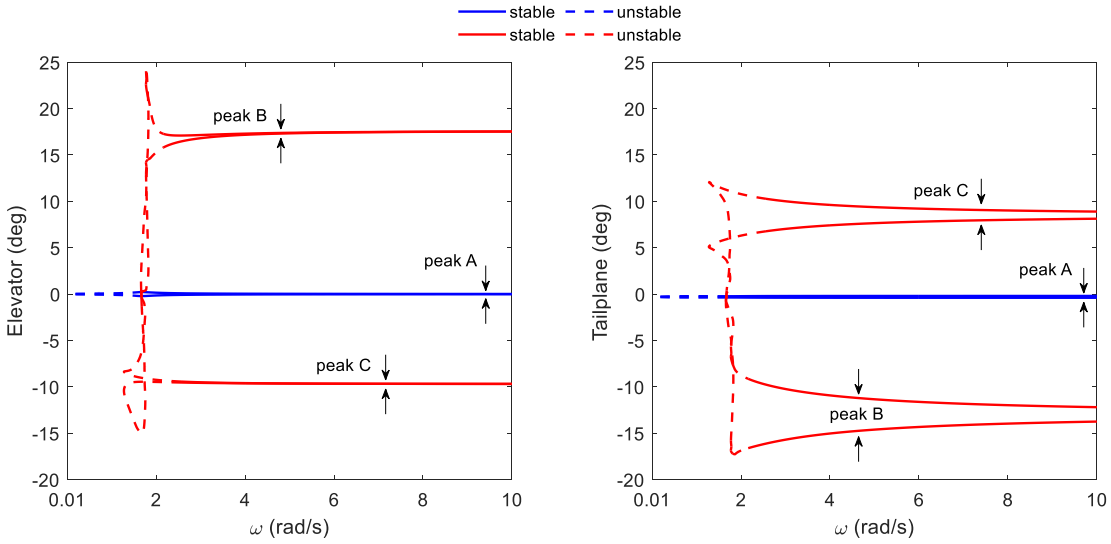

Fig. 7 Bifurcation diagrams: ω continuation. Solutions of the same branch are plotted in same colours.

When ω is sufficiently high (above 2.56 rad/s), there are three possible stable responses as indicated by the three labels A-C. These labels correspond to the three inflection points shown in Fig. 4, with A being the desirable one. In the presence of multiple stable solutions, the initial condition will dictate which solution the system converges to in the absence of any changes to inputs during the simulation. The continuation solver indicates that B and C are connected (shown as red) and can therefore be detected when the starting solution converges to either the B or C inflection point. Branch A, on the other hand, is not connected to the other two. Despite this, we have seen from Fig. 6b that the simulation converged to point C at ω = 4 rad/s – indicating that branch A becomes an increasingly weak attractor as ω reduces.

The existence of multiple solutions can also be seen at lower frequencies. To illustrate, Fig. 8 shows a magnified view of peak B at lower frequencies. We can see that there are at least two stable solutions on this branch alone at around 1.78 rad/s, which have been verified by time simulation (not shown).

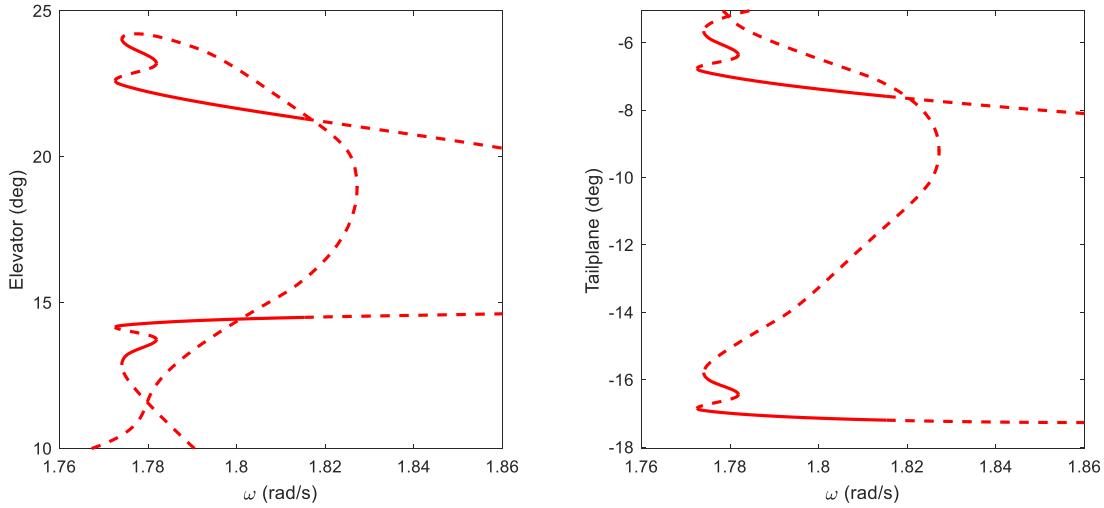

Fig. 8 Magnified view of peak B at low frequencies.

Results in this section have exemplified the potentially complex dynamics in a harmonically-forced system in general, and in an extremum-seeking controller in particular. Continuation not only provides a method to systematically characterise these behaviours, but can also be used to aid controller tuning via running a series of parameter sweeps. This argument has been made in previous studies on equilibrium bifurcation analysis (no harmonic forcing) [25], but it is even more important here because time simulations like those shown in Fig. 6 are even more computationally expensive to run due to the wide frequency separation between the forcing term and the plant's dynamics.

4.2 Multi-Harmonic Resonances

As discussed in section 1, it is not practical to maintain sufficient frequency separation in a harmonically-forced flight dynamics model in order to approximate the whole system as an equilibrium map. Numerical continuation is not subjected to such a restriction and therefore can potentially detect instances of resonances due to modal coupling between the aircraft's dynamic modes and the harmonic forcing terms. To illustrate, consider the aircraft trimmed for level flight at 1 deg angle of attack with both the manoeuvre-demand and the auto-trim controller active. The continuation parameter is now the proportional gain K_E, which is commonly referred to as the learning rate parameter. The resulting bifurcation diagram is shown in Fig. 9. Stability is lost at around K_E = 6 via a torus bifurcation. We compare the stable and unstable responses in Fig. 10 using two different values for K_E. It can be seen that for K_E = 6, a second frequency component has appeared with a frequency of 0.35 rad/s. This lies between the two natural frequencies of the aircraft: 0.10 rad/s for the phugoid mode and 1.50 rad/s for the short-period mode. It could therefore be inferred that although ω = 6 rad/s is higher that both natural frequencies, an internal resonance has occurred due to the high controller gain, leading to the multi-harmonic response observed in Fig. 10. This further underlines the advantage of the harmonically-forced technique.

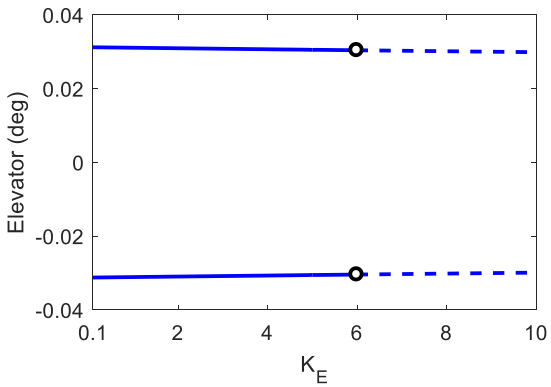

Fig. 9. Continuation in the learning rate gain at 1 deg angle of attack. The forcing frequency is 6 rad/s.

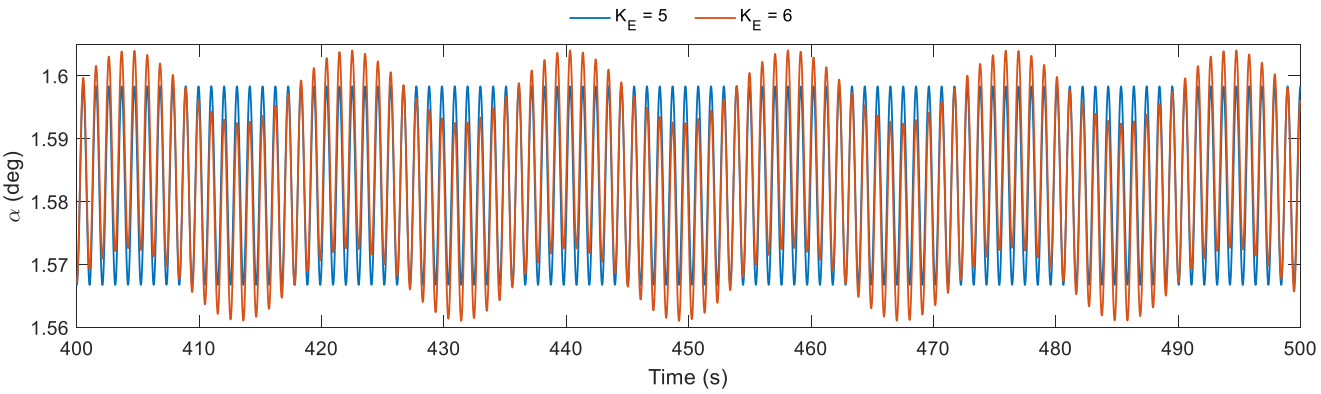

Fig. 10 Single- and multi-harmonic responses

5 Conclusion

The use of harmonically-forced bifurcation analysis to analyse a nonlinear extremum seeking controller has been presented. Our results have demonstrated that combining two approaches provides a powerful framework for analysing complex nonlinear extremum seeking systems where existing approximations can be mathematically impractical or restrictive. Further developments in the topic should explore a realistic example, which exemplifies both the capability of continuation as well as the advantages of the extremum seeking method.

Acknowledgements

We are grateful to NASA Langley Research Center, specifically Kevin Cunningham and Gautam Shah, for providing the GTT model.

References

1. Y. Tan, W. H. Moase, C. Manzie, D. Nešić, and I. M. Y. Mareels. Extremum seeking from 1922 to 2010. In *Proceedings of the 29th Chinese Control Conference*, 2010.

2. Miroslav Krstić, and Hsin-Hsiung Wang. Stability of extremum seeking feedback for general nonlinear dynamic systems. *Automatica*, 36(4), 2000.DOI: 10.1016/S0005-1098(99)00183-1

3. Wang Hsin-Hsiung, S. Yeung, and Miroslav Krstić. Experimental application of extremum seeking on an axial-flow compressor. *IEEE Transactions on Control Systems Technology*, 8(2), 2000.DOI: 10.1109/87.826801

4. Jui-Ho Chen, Her-Terng Yau, and Weir Hung. Design and study on sliding mode extremum seeking control of the chaos embedded particle swarm optimization for maximum power point tracking in wind power systems. *Energies*, 7(3), 2014.DOI: 10.3390/en7031706

5. Paolo Binetti, Kartik B. Ariyur, Miroslav Krstić, and Franco Bernelli. Formation flight optimization using extremum seeking feedback. *Journal of Guidance, Control, and Dynamics*, 26(1), 2003.DOI: 10.2514/2.5024

6. N. Killingsworth, and M. Krstić. Auto-tuning of pid controllers via extremum seeking. In *Proceedings of the 2005, American Control Conference, 2005.*, 2005.

7. Wang Hsin-Hsiung, and Miroslav Krstić. Extremum seeking for limit cycle minimization. *IEEE Transactions on Automatic Control*, 45(12), 2000.DOI: 10.1109/9.895589

8. Dragan Nešić. Extremum seeking control: Convergence analysis. *European Journal of Control*, 15(3), 2009.DOI: 10.3166/ejc.15.331-347

9. Mark Haring, Nathan van de Wouw, and Dragan Nešić. Extremum-seeking control for nonlinear systems with periodic steady-state outputs. *Automatica*, 49(6), 2013.DOI: doi.org/10.1016/j.automatica.2013.02.061

10. MathWorks. "*Simulink control design release notes*", https://uk.mathworks.com/help/slcontrol/release-notes.html [retrieved 21 February 2022].

11. Laurent Dewasme, and Alain Vande Wouwer. Model-free extremum seeking control of bioprocesses: A review with a worked example. *Processes*, 8(10), 2020.DOI: 10.3390/pr8101209

12. Kartik B. Ariyur, and Miroslav Krstić. *Real-time optimization by extremum-seeking control.* John Wiley & Sons, 2003.

13. Chunlei Zhang, and Raul Ordonez. *Extremum-seeking control and applications a numerical optimization-based approach.* Springer, 2012.

14. Olle Trollberg, Bengt Carlsson, and Elling W. Jacobsen. Extremum seeking control of the canon process—existence of multiple stationary solutions. *Journal of Process Control*, 24(2), 2014.DOI: 10.1016/j.jprocont.2013.11.007

15. Olle Trollberg, and Elling W. Jacobsen. On bifurcations of the zero dynamics - connecting steady-state optimality to process dynamics. In *IFAC-PapersOnLine*, 2015.

16. Olle Trollberg, and Elling W Jacobsen. "Non-uniqueness of stationary solutions in extremum seeking control," *arXiv preprint arXiv:1802.08520*. 2018.

17. Olle Trollberg. "On real-time optimization using extremum seeking control and economic model predictive control with applications to bioreactors and paper machines," *School of Electrical Engineering*. KTH Royal Institute of Technology, Stockholm, 2017.

18. Duc H. Nguyen, Mark H. Lowenberg, and Simon A. Neild. Frequency-domain bifurcation analysis of a nonlinear flight dynamics model. *Journal of Guidance, Control, and Dynamics*, 44(1), 2021.DOI: 10.2514/1.G005197

19. Duc H. Nguyen, M. H. Lowenberg, and S. A. Neild. Effect of actuator saturation on pilot-induced oscillation: A nonlinear bifurcation analysis. *Journal of Guidance, Control, and Dynamics*, 44(5), 2021.DOI: 10.2514/1.G005840

20. Yury Didenko, Alexander Dolotovsky, Sergey Gorelov, Valery Ivakha, Vladimir Motovilov, Alexey Tarasov, and Victor Chochiev. The specific features of fbw control laws of advanced regional jet. In *IFAC Proceedings Volumes*, 2007.

21. F Holzapfel, M Heller, M Weingartner, G Sachs, and O da Costa. Development of control laws for the simulation of a new transport aircraft. *Proceedings of the Institution of Mechanical Engineers, Part G: Journal of Aerospace Engineering*, 223(2), 2009.DOI: 10.1243/09544100jaero309

22. Dominik Niedermeier, and Anthony A. Lambregts. Fly-by-wire augmented manual control - basic design considerations. In *28th International Congress of the Aeronautical Sciences*, Brisbane, Australia, 2012.

23. R. Mehra, and J. Carroll. Bifurcation analysis of aircraft high angle-of-attack flight dynamics. In *6th Atmospheric Flight Mechanics Conference*, Danvers, MA, 1980.

24. James V. Carroll, and Raman K. Mehra. Bifurcation analysis of nonlinear aircraft dynamics. *Journal of Guidance, Control, and Dynamics*, 5(5), 1982.DOI: 10.2514/3.56198

25. Sanjiv Sharma, Etienne B. Coetzee, Mark H. Lowenberg, Simon A. Neild, and Bernd Krauskopf. Numerical continuation and bifurcation analysis in aircraft design: An industrial perspective. *Philosophical Transactions of the Royal Society A: Mathematical, Physical and Engineering Sciences,* 373(2051), 2015.DOI: doi:10.1098/rsta.2014.0406

26. C. C. Jahnke, and F. E. C. Culick. Application of bifurcation theory to the high-angle-of-attack dynamics of the f-14. *Journal of Aircraft,* 31(1), 1994.DOI: 10.2514/3.46451

27. Stephen J. Gill, Mark H. Lowenberg, Simon A. Neild, Luis G. Crespo, Bernd Krauskopf, and Guilhem Puyou. Nonlinear dynamics of aircraft controller characteristics outside the standard flight envelope. *Journal of Guidance, Control, and Dynamics,* 38(12), 2015.DOI: 10.2514/1.G000966

28. Stephen J. Gill, Mark H. Lowenberg, Simon A. Neild, Luis G. Crespo, and Bernd Krauskopf. Impact of controller delays on the nonlinear dynamics of remotely piloted aircraft. *Journal of Guidance, Control, and Dynamics,* 39(2), 2016.DOI: 10.2514/1.G001222

29. Etienne Coetzee, Bernd Krauskopf, and Mark H. Lowenberg. The dynamical systems toolbox: Integrating auto into matlab. In *16th US National Congress of Theoretical and Applied Mechanics*, State College, PA, 2010.

30. Eusebius J. Doedel. "*Auto-07p, continuation and bifurcation software for ordinary differential equations, ver. 07p*", http://www.macs.hw.ac.uk/~gabriel/auto07/auto.html [retrieved 21 February 2022].